Color Quality Comparison in Spectrally (*Un*)Correlated Random Field Models

Michal Havlíček

Institute of Information
Theory and Automation,
Czech Academy of
Sciences
Pod Vodarenskou vezi 4
182 08 Prague, Czechia
havlimi2@utia.cas.cz

Michal Haindl

Institute of Information
Theory and Automation,
Czech Academy of
Sciences
Pod Vodarenskou vezi 4
182 08 Prague, Czechia
haindl@utia.cas.cz

ABSTRACT

We inspect the ability to reproduce spectral (color) composition in random field-based texture models, test when it can neglect spectral correlation, and simplify these random models without visibly depreciating their visual quality. These probabilistic models present essential two or three-dimensional factors for modeling seven-dimensional Bidirectional Texture Function (BTF) - the most advanced representation currently used in real-world material visual properties modeling. They can seamlessly approximate original measured massive data and extend them to an arbitrary size or simulate unmeasured ones. Using extensive test data sets and a small set of setup control parameters, these models reach a vast compression ratio while maintaining the visual quality of measurements, and thus, they are the only viable alternative for BTF practical usage.

Keywords

Texture Analysis, Texture Synthesis, Texture Color Quality Comparison, Texture Modeling, BTF.

1 INTRODUCTION

Enhancing Photorealism in Virtual Reality (VR) scenes necessitates the meticulous application of textures that accurately depict natural material surfaces, ensuring a seamless fusion of visual elements. In the realm of computer graphics, achieving lifelike material appearances relies on visual textures, conceptualized as manifestations of a mathematically-defined random field (RF) possessing spatially uniform attributes. This texture model manifests as a discrete RF, comprising random vectors predominantly arranged on a rectangular lattice grid. The vector space's dimensionality corresponds to the spectral planes within the texture, delineating the richness and complexity of the visual representation.

Real-world materials exhibit intricate physical characteristics, with their micro-structures intricately influencing both reflectance and overall visual presentation. While imperceptible to the naked eye, these micro-structures significantly impact how materials reflect light under various viewing and illumination conditions. The most advanced representation currently available for quantifying and modeling these complexities is the Bidirectional Texture Function (BTF), introduced in [Dan97a]. BTF data serves as the most precise digital emulation of real-world material visual properties, offering analytical insights that elude alternative, less comprehensive visual measurement techniques. The BTF is a seven-dimensional function that encompasses four parameters related to illumination and viewing angles, including azimuthal and elevation angles, one parameter indexing spectral channels, and two parameters representing planar coordinates. This comprehensive model accurately preserves all visual effects inherent to natural materials, including self-occlusions, self-shadowing, inter-reflections, and sub-surface scattering, ensuring a faithful representation of real-world surfaces.

Numerous applications (automotive, airspace, safety, architecture, interior design, entertainment industry, movies, computer games, advertising, material recognition) [Hai06a, Sca09a, Vac09a, Vac10a] require to analyze or visualize real-world material visual properties. BTF data are the most advanced and accurate digital representation of real-world material visual properties to date, and their analysis provides information about the measured materials that mainly cannot be attained using any alternative visual measure-

ments or representations. Results of multidimensional textures-related research are also applicable to medical applications [Cul04a, Hai07a, Hai08b, Gri09a] and varied image processing problems, such as image restoration [Hai02a], cultural heritage preservation [Mal01a, Has11a]. Moreover, psychophysical studies of these data [Fil08a] have shown that analyzing of different BTF samples can help understand human perception of real-world materials.

BTF is represented by thousands of given material surface images taken in different combinations of light sources and observation positions during measurement. BTF data size can reach up to several terabytes [HFV12a] even for a limited number of combinations of illumination and viewing angles and small planar size of the measured material, usually several square centimeters [Hai13a]. These restrictions exclude the direct use of measured BTF in applications, and accordingly, some compression and enlargement are necessary. Two enlargement alternatives exist - sampling methods and mathematical models. Sampling methods require storing parts of the original measurements, cannot avoid seams, and offer a minimal compression ratio. Mathematical models generate unlimited enlarged versions of the original texture directly from their small fixed set of parameters, thus offering extreme data compression without seams but may compromise visual quality.

Such quality compromise is hard to express as fully automatic texture quality assessment and mutual similarity evaluation of two or more of them present a significant but complex problem that needs to be solved. Validation of the state-of-the-art texture fidelity criteria [Hai14a] based on the online benchmark [1] demonstrated that none of already published ones, i.e., CW-SSIM [Wan09a], (STSIM-1, STSIM-2, STSIM-M) [Zuj13a] can be reliably used for such task at all. Psycho-physical evaluations are a trustworthy alternative, but they are extremely impractical, expensive, and generally demanding. A pressing need is for a reliable criterion to support texture model development, which would be able to compare the original texture with synthesized or reconstructed ones and identify the best result and, therefore, corresponding optimal model parameter settings for specific models. Such criterion also plays a vital role in efficient content-based image retrieval, e.g., from digital libraries or multimedia databases.

This paper answers whether we can model a BTF texture using mathematical models on spectrally decorrelated data. We compare random fields-based texture models using their spectral quality, i.e., we investigate how individual models can represent color information

of the original data. We propose a novel criterion that allows us to predict when monospectral decorrelated channels can be modeled by a set of simpler 2D random fields and when fully spectrally correlated 3D models with more than $no\_spectral\_channels \times$ parameters are required compared to 2D models.

2 BTF RANDOM FIELD MODELS

The size of BTF data prohibits its direct integration into graphic applications, necessitating compression for practical usage. Additionally, BTF data is typically acquired under a limited set of illumination and viewing conditions, mandating reconstruction of the BTF space for real-world application. Furthermore, given the relatively small planar size of the measured sample from which BTF data originates, seamless texture enlargement becomes imperative. These essential considerations collectively fall under the umbrella of BTF modeling, which encompasses techniques to address the challenges posed by data size, reconstruction, and texture enlargement, ensuring effective utilization of BTF data in graphics applications. In addition to probabilistic BTF models, there is an alternative approach to approximate BTF data using pixel-wise generalizations of existing BRDF models, known as SVBRDF. However, this method comes with trade-offs, as it sacrifices visual quality by omitting critical features such as self-occlusions, self-shadowing, inter-reflections, and subsurface scattering. Furthermore, it cannot achieve the same level of compression efficiency as fully probabilistic BTF models, which offer significantly higher compression ratios and arbitrary size texture generation without visible discontinuities.

Modeling BTF based on probabilistic models necessitates the utilization of multi-dimensional models. However, such models are not prevalent and encounter various unresolved theoretical challenges, as noted in [Hai13a]. One potential workaround involves spectrally and spatially factorizing the BTF space, enabling its representation through a series of lower-dimensional models. Unfortunately, real data are correlated and can be spectrally factorized only approximately, which can lead to a loss of spectral information.

Using 2D models [Hai23a] for multi-spectral material data requires the input to be spectrally de-correlated using the Karhunen-Loève Transformation (KLT) so that resulting mono-spectral factors can be modeled independently. The 2D - 3D models compression ratio for the measured BTF space in our representation (6 561 measurements) is 1 : 19 683. However, this step leads to an inevitable loss of information. The approximation error is proportional to the extent of the color space contained in the modeled texture.

The original data space $\tilde{Y}$ is transformed into the new one with coordinate axes Y. The new basis consists

---

[1] http://tfa.utia.cas.cz

of the eigenvectors of the second-order statistical moments matrix $\Sigma = E\{\tilde{Y}_r \tilde{Y}_r^T\}$ where r denotes a multi-index $r = (r_1, r_2)$, $r \in I$, with the row and column indices, $\bullet$ all possible values of the corresponding index, I is a finite discrete 2D rectangular $M \times N$ index lattice, and d is the number of spectral bands. The projection of a $d \times 1$ random vector $\tilde{Y}_r$ onto the KLT coordinate system uses transformation matrix T, which consists of eigenvectors of Σ. If the measured data are Gaussian, then the transformed data are independent, and thus, each mono spectral factor can be modelled independently [Hai23a]. Although this assumption generally does not hold, practical results show that it may be taken into account without a significant impact on the visual quality of achieved results.

The texture pixels are defined as intensity values (2D) or intensity vectors (3D) on multiple finite $M \times N$ 2D lattice. The 3D multiindex is $r = \{r_1, r_2, r_3\}$ with spatial (r_1, r_2) and spectral (r_3) indices. For mathematical simplicity, all lattices are defined as double toroidal [Hai13a]. Markovian neighboring lattice locations are the set of relative lattice locations called Contextual Neighbourhood (CN) I_r. The selection of an appropriate CN influences the overall model performance: CN containing too few elements cannot capture all texture details. On the other hand, including the unnecessary elements adds to the computational burden and can degrade the model's performance as an additional noise source.

2.1 2D Causal Auto-Regressive Model

The Causal Auto-Regressive (CAR) RF is a collection of random variables with a joint probability density on the set of all possible realizations Y of the $M \times N$ lattice I [Hai23a]:

$$p(Y|\gamma, \sigma^{-2}) = (2\pi\sigma^2)^{-\frac{(MN-1)}{2}} \tag{1}$$
$$exp\left\{-\frac{1}{2}tr\left\{\sigma^{-2}\begin{pmatrix} -\alpha \\ \gamma^T \end{pmatrix}^T V_{MN-1} \begin{pmatrix} -\alpha \\ \gamma^T \end{pmatrix}\right\}\right\} \ ,$$

where α is a vector of unities, $\gamma = [a_1, \ldots, a_\eta]$ is a parameter vector, η denotes the cardinality of a causal contextual neighbourhood I_r^C, σ is variance of Gaussian distribution and

$$V_{t-1} = \tilde{V}_{t-1} + V_0 = \begin{pmatrix} \tilde{V}_{yy(t-1)} & \tilde{V}_{xy(t-1)}^T \\ \tilde{V}_{xy(t-1)} & \tilde{V}_{xx(t-1)} \end{pmatrix} + V_0 \ , \tag{2}$$

$$\tilde{V}_{xx(t-1)} = \sum_{k=1}^{t-1} X_k X_k^T \qquad \tilde{V}_{xy(t-1)} = \sum_{k=1}^{t-1} X_k Y_k^T \ ,$$
$$\tilde{V}_{yy(t-1)} = \sum_{k=1}^{t-1} Y_k Y_k^T \qquad X_k = [Y_{k-s}^T : \forall s \in I_k^C]^T \ .$$

Simplified notation $t, t-1, \ldots$ denotes the process position in I, i.e., t is the index of the sequence of multi-indices $((r_1, r_2)_t)_{t=1}^{MN}$. The order of indices $(r_1, r_2) = r$ depends on the order in which the analyzed texture pixels are processed. The data from model history obtained during adaptation are denoted as $Y_{(t-1)}$. For the sake of proper model adaptation, the standard exponential forgetting factor technique can be utilized [Hai23a]. The 2D CAR model can be expressed as a stationary causal uncorrelated noise driven 2D auto-regressive process with correlation structure [Hai23a]:

$$E\{e_r e_s\} = \begin{cases} \sigma_i^2 & s = r, \\ 0 & otherwise. \end{cases} \tag{3}$$

Unlike 2D Gaussian Markov random field model, the parameters of 2D CAR model can be estimated analytically without simplifying approximations using the maximum likelihood, the LS or Bayesian methods [Hai02c]. The Bayesian parameter estimations of the model with the normal-Wishart parameter prior which maximizes the posterior density are [Hai23a]:

$$\hat{\gamma}_{t-1}^T = V_{xx(t-1)}^{-1} V_{xy(t-1)} \ , \tag{4}$$
$$\hat{\sigma}_{t-1}^2 = \frac{\lambda_{(t-1)}}{\beta(t)} \ , \tag{5}$$
$$\lambda_{(t-1)} = V_{yy(t-1)} - V_{xy(t-1)}^T V_{xx(t-1)}^{-1} V_{xy(t-1)} \ , \tag{6}$$
$$\beta(t) = \beta(0) + t - 1, \ \beta(0) > 1 \ , \tag{7}$$

and $V_{xx(0)}$, $V_{xy(0)}$, $V_{yy(0)}$ are from normal-gamma parameter prior. The 2D CAR synthesis can be easily performed [Hai23a].

2.2 3D Causal Auto-Regressive Model

The 3D CAR RF is a collection of random variables with a joint probability density on the set of all possible realizations Y of the $M \times N \times d$ lattice I, subject to the condition [Hai23a]:

$$p(Y|\Theta, \Sigma^{-1}) = 2\pi^{-\frac{d(MN-1)}{2}} |\Sigma^{-1}|^{\frac{MN-1}{2}} \tag{8}$$
$$exp\left\{-\frac{1}{2}tr\left\{\Sigma^{-1}\begin{pmatrix} -I \\ \Theta^T \end{pmatrix}^T V_{MN-1} \begin{pmatrix} -I \\ \Theta^T \end{pmatrix}\right\}\right\} \ ,$$

where I is identity matrix, Σ is covariance matrix of Gaussian distribution and Θ is $d \times d\eta$ parameter matrix $\Theta = (A_1, \ldots, A_\eta)$ where $\forall i \in \{1, \ldots, \eta\}$ [Hai23a]:

$$A_i = \begin{pmatrix} a_{1,1}^i & \cdots & a_{1,d}^i \\ \vdots & \ddots & \vdots \\ a_{d,1}^i & \cdots & a_{d,d}^i \end{pmatrix} \ . \tag{9}$$

The 3D CAR model can be expressed as a stationary causal uncorrelated noise driven 3D auto-regressive process [Hai23a]:

$$Y_r = \Theta X_r + e_r \ , \tag{10}$$

with correlation structure [Hai13a]:

$$E\{e_r e_s\} = \begin{cases} \Sigma & s = r, \\ 0 & otherwise, \end{cases} \quad (11)$$

The estimates of model parameters are [Hai23a]:

$$\hat{\Theta}_{t-1}^T = V_{xx(t-1)}^{-1} V_{xy(t-1)} \;, \quad (12)$$

$$\hat{\Sigma}_{t-1} = \frac{\lambda_{(t-1)}}{\beta(t)} \;. \quad (13)$$

where $V_{xx(0)}$, $V_{xy(0)}$, $V_{yy(0)}$ are from normal-Wishart parameter prior. The model can be directly generated from the model equation (10).

2.3 Moving Average Model

2D MA texture model assumes that the modeled mono spectral factor is an output of a specific underlying system that completely characterizes it in response to a 2D uncorrelated random input, and that is a sample from 2D RF defined on an infinite 2D lattice. The impulse response of a linear 2D filter can represent this system. Therefore, a convolution of an uncorrelated 2D RF can generate the mono spectral factor with this 2D filter.

Supposing that the mono spectral factor Y is the output of the underlying linear system which completely characterizes it in response to the 2D uncorrelated random input e_r, then $Y_{r,i}$ is determined by the following difference equation [Li92a]:

$$Y_{r,i} = \sum_{s \in I_r} a_{s,i}\, e_{r-s,i} \;, \quad (14)$$

where a_s are constant coefficients. I_r determines the causality or non-causality of the model.

To fit the model to a given mono spectral factor Y, the parameters a_s have to be estimated. This may be done using a method [Li92a] similar to the one-dimensional (1D) Random Decrement Technique [Col73a]. The estimation procedure begins by arbitrarily selecting a threshold ξ usually chosen as some percentage of the standard deviation of the intensity values of the mono spectral factor. Generally, higher value of ξ leads to the synthesized textures with higher contrast and vice versa. Unfortunately, there does not exist any method for an automatic determination of the optimal value of ξ, i.e., the value at which the result that is visually the most similar to the original is achieved.

During the model parameter estimation process every pixel of the analyzed mono spectral factor is examined. If the intensity value of the examined pixel Y_r is higher than the value of the threshold ξ and among the four adjacent pixels to the pixel Y_r at least one in the same row and at least one in the same column are lower than ξ, i.e., $Y_{(r_1,r_2)} > \xi$ and ($Y_{(r_1,r_2-1)} < \xi$ or $Y_{(r_1,r_2+1)} < \xi$

and $Y_{(r_1-1,r_2)} < \xi$ or $Y_{(r_1+1,r_2)} < \xi$) holds then the pixel Y_r is referred to as significant. For each significant pixel Y_r, the intensity values of pixels whose pixel-relative position to Y_r is defined by I_r form a vector Υ of length which equals the number of elements of I_r. It is assumed that there is a unambiguous correspondence between components of Υ, parameters a_s and the elements of I_r. Vectors Υ_υ of all significant pixels of Y are summed and divided by the number of significant pixels (g) to obtain the estimate of the model parameters, i.e., [Li92a]:

$$\hat{a}_s = \frac{1}{g} \sum_{\upsilon=1}^{g} \Upsilon_\upsilon \;. \quad (15)$$

The model assumes that the modelled texture is the RF realization with zero mean therefore, it is necessary to estimate the mean value of the pixel intensity levels. Estimated mean value is saved together with estimated model parameters for the texture synthesis purposes.

2D MA texture model is able to generate synthetic mono spectral factor of arbitrary size from the model parameters a_s according to the model equation (14). It has been proven that the result of the synthesis closely approximates the first and second order statistics of the original when e_r is the white noise [Li92a].

2.4 Extended Moving Average Model

It is possible to extend the approach described in Sec. 2.3 to obtain 3D MA texture model as suggested in [Hav15a]. Using a 3D model avoids spectral de-correlation of analyzed multi-spectral texture with possible loss of certain portion of the information which is a certain advantage over the 2D MA texture model. The 3D MA texture model assumes that the input is a stochastic multi-spectral texture and the output of certain underlying system which completely characterizes it in response to a 3D uncorrelated random input $e_{r,i}$. 3D MA model equation represents an extended version of (14) allowing simultaneous modelling of all texture spectral planes. $Y_{r,i}$ is determined by the following difference equation [Hav15a]:

$$Y_{r,i} = \sum_{j=1}^{d} \sum_{s \in I_r} a_{s,i,j}\, e_{r-s,i} \;, \quad (16)$$

where $a_{s,i,j}$ are constant coefficients. The geometry of I_r determines the causality or non-causality of the model.

Parameters $a_{s,i,j}$ have to be estimated to fit the model equation (16) to certain multi-spectral texture Y performing extended variant of the method used for 2D MA texture model parameter estimation. The estimation procedure begins by selecting thresholds ξ_k, $k \in$

$\{1, \ldots, d\}$, usually chosen as some percentage of the standard deviation of the pixel intensity values of the corresponding spectral planes. Generally, higher values of ξ_k leads to the synthesized textures with higher contrast and vice versa. For simplicity and possible comparison with 2D MA, all ξ_k were set equal and denoted ξ there. There does not exist any method for an automatic determination of the optimal values of ξ_k, i.e., the value at which the result that is visually the most similar to the original is achieved.

During the model parameter estimation process every pixel of the analyzed multi-spectral texture is examined. Individual parameters $a_{s,i,j}$ are estimated independently but at the same time. If $Y_{(r_1,r_2),i} > \xi_i$ and ($Y_{(r_1,r_2-1),j} < \xi_j$ or $Y_{(r_1,r_2+1),j} < \xi_j$ and $Y_{(r_1-1,r_2),j} < \xi_j$ or $Y_{(r_1+1,r_2),j} < \xi_j$) holds then the pixel Y_r is referred to as significant for $a_{s,i,j}$. For each significant pixel Y_r for $a_{s,i,j}$, the intensity values in j-th spectral plane of pixels whose pixel-relative position to Y_r is defined by I_r form a vector Υ^{ij} of length which equals the number of elements of I_r. It is assumed that there is a unambiguous correspondence between components of Υ^{ij}, parameters $a_{s,i,j}$ and the elements of I_r. Vectors Υ_v^{ij} of all pixels significant for $a_{s,i,j}$ are summed and divided by their number (denoted as g^{ij}) to obtain the estimate of the model parameters, i.e., [Hav15a]:

$$\hat{a}_{s,i,j} = \frac{1}{g^{ij}} \sum_{v=1}^{g^{ij}} \Upsilon_v^{ij} \ . \tag{17}$$

The model assumes that the modelled multi-spectral texture is the RF realization with zero mean therefore, it is necessary to estimate the mean value of the pixel intensity levels of individual spectral planes.

The 3D MA model is able to generate synthetic multi-spectral texture of arbitrary size from the model parameters $a_{s,i,j}$ according to (16).

2.5 Multi-Spectral Simultaneous Auto-Regressive Model

The Multi-Spectral Simultaneous Auto-Regressive (MSAR) model [Hai12a] is based on the (MSAR) texture model [Ben98a]. The MSAR model can be expressed as a stationary, non-causal correlated noise-driven 3D auto-regressive process [Ben98a]:

$$Y_{r,i} = \sum_{j=1}^{d} \sum_{s \in I_r^{ij}} a_{s,i,j} Y_{r \oplus s,j} + \sqrt{\sigma_i} \varepsilon_{r,i} \ , \tag{18}$$

where I_r^{ij} denotes the CN relating intensity values in the i-th spectral plane to the neighbouring ones in the j-th ($j \in \{1, \ldots, d\}$) spectral plane, $a_{s,i,j}$ are the corresponding parameters which define the dependence of $Y_{r,i}$ on its neighbours defined by I_r^{ij}. Symbol $\oplus$

denotes modulo addition in each index of the multi-indices r, i.e., modulo addition of M for r_1 and modulo addition of M for r_2 and $s = (s_1, s_2)$. The driving noise $\varepsilon_{r,i}$ are i.i.d. random variables distributed normally with zero mean and constant but unknown variance σ_i. Rewriting (18) in matrix form the MSAR model equations become [Ben98a]:

$$\Psi Y = \varepsilon \ , \tag{19}$$

$$\Psi = \begin{pmatrix} \Psi_{11} & \Psi_{12} & \ldots & \Psi_{1d} \\ \Psi_{21} & \Psi_{22} & \ldots & \Psi_{2d} \\ \vdots & \vdots & \ddots & \vdots \\ \Psi_{d1} & \Psi_{d2} & \ldots & \Psi_{dd} \end{pmatrix} \ , \tag{20}$$

$$Y = \{Y_1, Y_2, \ldots, Y_d\}^T \ , \tag{21}$$

$$\varepsilon = \{\sqrt{\sigma_1}\varepsilon_1, \sqrt{\sigma_2}\varepsilon_2, \ldots, \sqrt{\sigma_d}\varepsilon_d\}^T \ , \tag{22}$$

where both Y_i and ε_i are vectors of length $M \times N$ of lexicographic ordered arrays of $Y_{r,i}$ and $\varepsilon_{r,i}$, respectively, i.e., $Y_i = \{Y_{(1,1),i}, Y_{(1,2),i}, \ldots, Y_{(1,M),i}, Y_{(2,1),i}, Y_{(2,2),i}, \ldots, Y_{(M,M),i}\}$ and similarly for ε_i. The transformation matrix Ψ is composed of $M^2 \times M^2$ block circulant sub-matrices [Ben98a]:

$$\Psi_{ij} = \begin{pmatrix} \Psi_{ij}^1 & \Psi_{ij}^2 & \ldots & \Psi_{ij}^M \\ \Psi_{ij}^M & \Psi_{ij}^1 & \ldots & \Psi_{ij}^{M-1} \\ \vdots & \vdots & \ddots & \vdots \\ \Psi_{ij}^2 & \Psi_{ij}^3 & \ldots & \Psi_{ij}^1 \end{pmatrix} \ , \tag{23}$$

where each element $\Psi_{ij}^k, k \in \{1, \ldots, M\}$, is an $M \times M$ circulant matrix whose (m,n)-th element is given by [Ben98a]:

$$\Psi_{i,j}^k(m,n) = \begin{cases} 1, & i = j, m = n, k = 1, \\ -a_{s,i,j}, & s_1 = k - 1, \\ & s_2 = ((n - m) \bmod M), \\ & (s_1, s_2) \in I_r^{ij}, \\ 0, & otherwise. \end{cases} \tag{24}$$

Rewriting (19) as $Y = \Psi^{-1}\varepsilon$, the covariance matrix is obtained as [Ben98a]:

$$\Sigma_Y = E\{\Psi^{-1} \varepsilon\varepsilon^T \Psi^{-T}\} = \Psi^{-1}\Sigma_\varepsilon\Psi^{-T} \tag{25}$$

$$\Sigma_\varepsilon = E\{\varepsilon\varepsilon^T\} = \begin{pmatrix} \sigma_1 I & 0 & \ldots & 0 \\ 0 & \sigma_2 I & \ldots & 0 \\ \vdots & \vdots & \ddots & \vdots \\ 0 & 0 & \ldots & \sigma_d I \end{pmatrix} \tag{26}$$

where I is the identity matrix. The positive definite property required of Σ_Y is ensured if Ψ is nonsingular. MSAR model parameters can be estimated using the Least Square (LS) approach. The estimate of the MSAR model parameters is obtained by equating the intensity values in individual pixel spectral planes of the analyzed texture to the expected ones predicted by the

model, leading to the independent systems of equations [Ben98a]:

$$Y_{r,i} = E\{Y_{r,i}|\gamma_i\} = X_{r,i}^T\gamma_i \ , \tag{27}$$

$$\gamma_i = [\gamma_{i1}, \gamma_{i2}, \ldots, \gamma_{id}]^T \ , \tag{28}$$

$$X_{r,i} = \left[\{Y_{r\oplus s,1} : s \in I_r^{i1}\}, \ldots, \{Y_{r\oplus s,d} : s \in I_r^{id}\}\right]^T \tag{29}$$

where $\gamma_{ij} = [a_{s,i,j} : \forall s \in I_r^{ij}]$. The LS solution $\hat{\gamma}_i$ and $\hat{\sigma}_i$ can be found as [Ben98a]:

$$\hat{\gamma}_i = \left(\sum_{r\in I} X_{r,i}X_{r,i}^T\right)^{-1}\left(\sum_{r\in I} X_{r,i}Y_{r,i}\right) \ , \tag{30}$$

$$\hat{\sigma}_i = \frac{1}{M^2}\sum_{r\in I}(Y_{r,i} - \hat{\gamma}_i^T X_{r,i})^2 \ . \tag{31}$$

The model assumes that the modeled texture is the RF realization with zero means; therefore, estimating the mean value of the pixel intensity levels of individual spectral planes is necessary. There are several possibilities existing for the MSAR texture model synthesis. Considering the double toroidal boundary conditions, the Discrete Fast Fourier Transform (DFFT) is the most effective method. The MSAR model equations (18) may be expressed in terms of the Discrete Fourier Transform (DFT) of each spectral plane as [Ben98a]:

$$\tilde{Y}_{t,i} = \sum_{j=1}^{d}\sum_{s\in I_r^{ij}} a_{s,i,j}\tilde{Y}_{t,j}e^{\sqrt{-1}\omega_{st}} + \sqrt{\sigma_i}\tilde{\varepsilon}_{t,i} \ , \tag{32}$$

where $\tilde{Y}_{t,i}$ and $\tilde{\varepsilon}_{t,i}$ are the 2D DFT coefficients of $Y_{r,i}$ and $\varepsilon_{r,i}$, respectively, at the discrete frequency index $t = (m,n)$ and $\omega_{st} = \frac{2\pi(ms_1+ns_2)}{M}$. The equations (32) can be written in matrix form as [Ben98a]:

$$\tilde{Y}_t = \Lambda_t^{-1}\Sigma^{\frac{1}{2}}\tilde{\varepsilon}_t, \ , \tag{33}$$

$$\tilde{Y}_t = \{\tilde{Y}_{t,1}, \tilde{Y}_{t,2}, \ldots, \tilde{Y}_{t,d}\}^T \ , \tag{34}$$

$$\tilde{\varepsilon}_t = \{\tilde{\varepsilon}_{t,1}, \tilde{\varepsilon}_{t,2}, \ldots, \tilde{\varepsilon}_{t,d}\}^T \ , \tag{35}$$

where the matrices Σ and Λ_t are defined as [Ben98a]:

$$\Sigma = \begin{pmatrix} \sigma_1 & 0 & \ldots & 0 \\ 0 & \sigma_2 & \ldots & 0 \\ \vdots & \vdots & \ddots & \vdots \\ 0 & 0 & \ldots & \sigma_d \end{pmatrix} \ , \tag{36}$$

$$\Lambda_t = \begin{pmatrix} \lambda_{t,11} & \lambda_{t,12} & \ldots & \lambda_{t,1d} \\ \lambda_{t,21} & \lambda_{t,22} & \ldots & \lambda_{t,2d} \\ \vdots & \vdots & \ddots & \vdots \\ \lambda_{t,d1} & \lambda_{t,d2} & \ldots & \lambda_{t,dd} \end{pmatrix} \ , \tag{37}$$

$$\lambda_{t,ij} = \begin{cases} 1 - \sum_{s\in I_r^{ij}} a_{s,i,j}\,e^{\sqrt{-1}\omega_{st}} & i = j, \\ -\sum_{s\in I_r^{ij}} a_{s,i,j}\,e^{\sqrt{-1}\omega_{st}} & i \neq j. \end{cases} \tag{38}$$

The MSAR model will be stable and valid if Λ_t is a non-singular matrix $for\ t \in I$. A $M \times M$ texture can

be synthesized from the estimated model parameters according to the following algorithm [Ben98a]:

1) Generate d noise 2D arrays $\varepsilon_{r,i}$ using a pseudo random number generator.

2) Calculate the 2D DFFT of each noise array separately.

3) For each discrete frequency index t compute: $\tilde{Y}_t = \Lambda_t^{-1}\Sigma^{\frac{1}{2}}\tilde{\varepsilon}_t$.

4) Perform the 2D inverse DFFT of each $\tilde{Y}_{t,i}$ separately.

2.6 Multi-Spectral Markov Random Field Model

The BTF Multi-Spectral Markov Random Field (BTF-MMRF) model is based on (MMRF) factor texture model [Ben98a]. A multi-spectral texture can be considered Markovian with respect to I_r^{ij} if it has following property [Ben98a]:

$$p(Y_{r,i}|Y_{s,j}, \forall j \in \{1,\ldots,d\} : j \neq i, \forall s \in I_r^{ij} : s \neq r)$$
$$= p(Y_{r,i}|Y_{s,j}, \forall j \in \{1,\ldots,d\}, \forall s \in I_r^{ij}) \ . \tag{39}$$

As the conditional distributions of $Y_{r,i}$ given $\{Y_{s,j}, \forall j \in \{1,\ldots,d\} : j \neq i, \forall s \in I_r^{ij} : s \neq r\}$ and $Y_{r,i}$ given $\{Y_{s,j}, \forall j \in \{1,\ldots,d\}, \forall s \in I_r^{ij}\}$ are the same, the best linear estimator of Y can be written as [Ben98a]:

$$Y_{r,i} = \sum_{j=1}^{d}\sum_{s\in N_r^{ij}} a_{s,i,j}Y_{r\oplus s,j} + \varepsilon_{r,i}, \ , \tag{40}$$

where $a_{s,i,j}$ are taken as the coefficients of the Minimum Mean Square Error (MMSE) estimate of $Y_{r,i}$ and $\varepsilon_{r,i}$ denotes the estimation error. From the orthogonality property of the MMSE estimates [Ben98a]:

$$E\{Y_{r,i}\varepsilon_{s,j}\} = \begin{cases} \sigma_i & i = j, s = r \ , \\ 0 & \text{otherwise} \ , \end{cases} \tag{41}$$

the correlation structure of the stationary noise $\varepsilon_{r,i}$ is [Ben98a]:

$$\Psi_{ij}^s = E\{\varepsilon_{r,i}\varepsilon_{r\oplus s,j}\} = \begin{cases} -a_{s,i,j}\sigma_j & s \in I_r^{ij} \ , \\ \sigma_j & s = 0, i = j, \\ 0 & \text{otherwise} \ . \end{cases} \tag{42}$$

Because the correlation functions have the symmetry property $\Psi_{ij}^s = \Psi_{ji}^{-s}$, there is an implicit requirement that I_r^{ij} and the associated coefficients are symmetric, i.e., $s \in I_r^{ij} \iff -s \in I_{-r}^{ji}$ and $\sigma_j\Psi_{ij}^s = \sigma_i\Psi_{ji}^{-s}$. Equation (40) can be rewritten in matrix form as: $\Psi Y = \varepsilon$ and equations (41) and (42) can be expressed using matrix notations as [Ben98a]:

$$\Sigma_\varepsilon = E\{Y\varepsilon^T\} = \begin{pmatrix} \sigma_1 I & 0 & \ldots & 0 \\ 0 & \sigma_2 I & \ldots & 0 \\ \vdots & \vdots & \ddots & \vdots \\ 0 & 0 & \ldots & \sigma_d I \end{pmatrix} \tag{43}$$

$$\Sigma_e = E\{\varepsilon\varepsilon^T\} = E\{\Psi Y\varepsilon^T\} = \Psi\Sigma_\varepsilon \ . \tag{44}$$

The model parameters must be chosen such that Σ_e is positive definite. Using (19) and (44), the MMRF covariance matrix can be found as [Ben98a]:

$$
\begin{aligned}
\Sigma_Y & = E\{YY^T\} = E\{\Psi^{-1}\varepsilon\varepsilon^T\Psi^{-T}\} \\
& = \Psi^{-1}\Sigma_e\Psi^{-T} = \Psi^{-1}\Sigma_\varepsilon \ . \qquad (45)
\end{aligned}
$$

Matrix Σ_Y will be admissible covariance matrix if all model parameters are chosen such that Σ_Y is positive definite which is consistent with the requirement that matrix Σ_e be positive definite, since $\Sigma_Y = \Sigma_\varepsilon\Sigma_e^{-1}\Sigma_\varepsilon$. MMRF model parameters can be estimated using an approach based on the LS method similar to the MSAR model parameter estimation. Due to the symmetry property of (42), the LS estimates are inherently nonlinear, and it is necessary to solve for all model parameters simultaneously. As in the case of the MSAR model parameter estimation, LS estimates are obtained by equating each pixel spectral intensity value to the expected value of one of the model equations. An iterative approach can be used to obtain the LS solutions [Ben98a]:

$$
\widehat{\gamma}_{i,t+1} = \left(\sum_{r\in I} Q_{r,i,t}Q_{r,i,t}^T\right)^{-1}\left(\sum_{r\in I} Q_{r,i,t}Y_{r,i}\right) \ , \qquad (46)
$$

$$
\widehat{\sigma}_{i,t+1} = \frac{1}{M^2}\sum_{r\in I}(Y_{r,i} - Q_{r,i,t}^T\widehat{\gamma}_{i,t})^2 \ , \qquad (47)
$$

$$
Q_{r,i,t} = \begin{pmatrix}
q_{r,11} & q_{r,12} & \dots & 0 & 0 \\
0 & \frac{\widehat{\sigma}_{2,t}q_{s,21}}{\widehat{\sigma}_{1,t}} & 0 & \dots & 0 \\
\vdots & \vdots & \vdots & \vdots & \vdots \\
0 & 0 & 0 & \frac{\widehat{\sigma}_{d,t}q_{r,dd-1}}{\widehat{\sigma}_{d-1,t}} & q_{r,dd}
\end{pmatrix}^T ,
$$

$$
q_{r,ij} = \begin{cases}
\{Y_{(r\oplus s),j} + Y_{(r\oplus -s),j} : s \in N_r^{ij}\} & i = j, \\
\{Y_{(r\oplus s),j} : s \in I_r^{ij}\} & i < j, \\
\{Y_{(r\oplus -s),j} : s \in I_r^{ij}\} & i > j,
\end{cases}
$$

with $\frac{\widehat{\sigma}_{z,1}}{\widehat{\sigma}_{z-1,1}} = 1, z \in (2,\dots,d)$, where $t \in \{1,\dots,+\infty\}$ denoting the order of the iteration. Although no proof of convergence exists for this procedure, experimental results indicate that a sufficiently accurate estimate is achieved in less than ten iterations. If the results of two consecutive iterations are the same within the achievable accuracy of the rounding on the used system, then such results are considered sufficiently accurate estimates. It should be noted that the LS estimate represents only a very rough approximation of the MMRF model parameter estimate. The algorithm for the synthesis of the MMRF model is identical to that one for the MSAR model, except the calculations in the third step which replaces citeBen97a: $\tilde{Y}_t = \Lambda_t^{-1}(\Lambda_t\Sigma)^{\frac{1}{2}}\tilde{\varepsilon}_t$. The MMRF model will exist and be stable if $\Lambda_t\Sigma$ is positive definite $\forall t \in I$.

2.7 Pseudo Markov Random Field Model

The BTF Pseudo Markov Random Field (BTF-PMRF) model [Hav12a] is based on the (PMRF) texture model [Ben98a]. The PMRF model represents an approximation of the MMRF model. The apparent motivation for deriving this approximation was to avoid an iterative parameter estimation method. The PMRF model was derived from the MMRF model by subtly modifying the correlation structure given in (42). The PMRF and the MMRF model equations are identical with one exception: the PMRF stationary noise $e_{r,i}$ is assumed to have the following correlation structure [Ben98a]:

$$
E\{\varepsilon_{r,i}\varepsilon_{s\oplus r,j}\} = \begin{cases}
-a_{s,i,j}\sqrt{\sigma_i\sigma_j} & s \in I_r^{ij}, \\
\sigma_j & s = 0, i = j, \\
0 & otherwise.
\end{cases} \qquad (48)
$$

The main difference between the MMRF model and the PMRF model and the significant advantage of the PMRF model is the fact that the estimate $\widehat{\gamma}$ is linear and independent of the estimate $\widehat{\sigma}$. The LS estimates of the PMRF model parameters are the same as those of the MMRF model, for $t = 1$. Therefore, the model parameter estimation does not require an iterative process, unlike the case of the MMRF model parameter estimation, which reduces the computational burden. Employing the same method used for the MMRF model synthesis in the case of the PMRF model, the calculations in the third step of the synthesis procedure become [Ben98a]: $\tilde{Y}_t = \Lambda_t^{-1}\Sigma^{\frac{1}{2}}\Lambda_t^{\frac{1}{2}}\tilde{\varepsilon}_t$. The PMRF model will exist and be stable if Λ_t is positive definite $\forall t \in I$.

3 COLOR QUALITY CRITERIA

3.1 Spectral Decorrelation Criterion

$$
\kappa(c_{\max}) = \frac{1}{c_{\max}^n}\det(\Sigma) \ , \qquad (49)
$$

where Σ is a $n \times n$ material texture spectral covariance matrix, $c_{\max}$ is the maximal possible spectral value per channel. If the criterion $\kappa(c_{\max}) \leq 3$, we can replace a 3D random field model with its Karhunen-Loeve decorrelated version and model each decorrelated single spectral band with a 2D random field model without significant MEMD error (50), i.e., with negligible color loss.

3.2 Color Composition Comparison

The Mean Exhaustive Minimum Distance (MEMD) [Hav19a] is used to compare the spectral composition of two textures and the cardinalities of the same colors but ignoring the locations of individual pixels. The comparison is performed by individually taking pixels from the first image and searching for the most similar, i.e., the closest in certain vector metric sense, to the ones in the second image. The pixel from the second

image identified as the most similar is removed from the stack representing the second image, and the local spectral error is recorded. The MEMD criterion is as follows:

$$\zeta(A,B) = \frac{1}{M} \sum_{(r_1,r_2)\in\langle A\rangle} \min_{(\acute{r}_1,\acute{r}_2)\in N} \left\{ \rho\left(Y^A_{r_1,r_2,\bullet}, Y^B_{\acute{r}_1,\acute{r}_2,\bullet}\right) \right\} ,$$

(50)

where $M = \min\left\{\sharp\{A\}, \sharp\{B\}\right\}$, $\sharp\{A\}$ is the number of pixels in A and similarly for $\sharp\{B\}$, $\min\{\emptyset\} = 0$, (r_1,r_2) denotes the location in A, $\langle A\rangle$ represents the set of all pixel indices of A, $(\acute{r}_1,\acute{r}_2)$ is the location in B, N is the set of unprocessed pixel indices of B, ρ is an arbitrary vector metric and $Y^A_{r_1,r_2,\bullet}$ represents the pixel at (r_1,r_2) in A, where $\bullet$ denotes all corresponding spectral indices, similarly for $Y^B_{\acute{r}_1,\acute{r}_2,\bullet}$. The term $\zeta(A,B)$ is evaluated using raster scanning of A. The algorithm stops when all pixels of A are scanned, or N becomes an empty set (see details in [Hav19a, Hav21a, Hav23a]).

4   TEST DATA

We used BTF MAM2014 Dataset [2] [Fil18a]. This dataset consists of 16 BTF of materials presented at the Workshop on Material Appearance Modelling (MAM) 2014. The BTF datasets consist of a collection of material images taken for lighting and viewing directions with an angular sampling of 81×81. The uncompressed HDR data (32-bit float) are represented in CIE XYZ colorspace. The spatial resolution of the datasets is 353.3 dpi. They included widely different natural, artificial, matte or glossy materials are mica, sand-fine, sand-coarse, burlap, cork, towel, green cloth, green felt, basketball, flocked paper, silver gold, brown tile, glass tile, blue-black-gold tile, crinkle paper, and basketweave. This texture set is illustrated in Fig. 1.

5   RESULTS

We used the same setup for all tested models, i.e., the number and type of used neighborhood sets. Using 16 BTF materials, each consisting of 6,561 images, testing ten random field models, and trying eight different neighborhood sets, each with three different Gaussian-Laplacian pyramid setups, we created 20,155,392 synthesized images, which were all compared with corresponding original data in total. The best result, i.e., the synthesized image most similar to the original using the MEMD criterion, was identified, and its corresponding MEMD value was used for the presented statistics. The mean MEMD of the best results and standard deviation for each tested model are counted for individual used materials and the whole test set. The results are the mean difference from original data in %
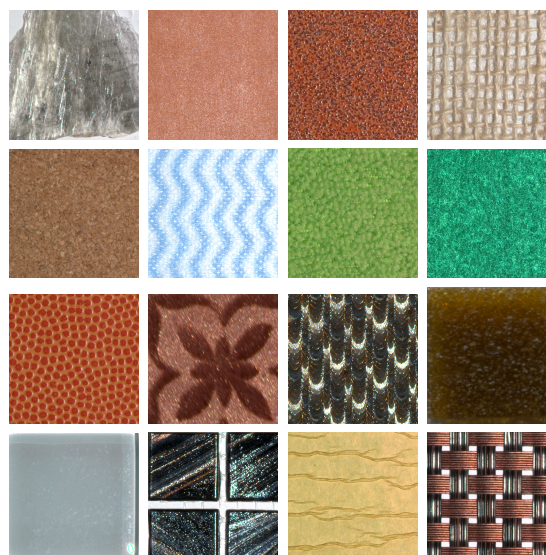
Figure 1: BTF MAM204 Dataset presentation (from upper-left to bottom-right): mica, sand-fine, sand-coarse, burlap, cork, towel, green cloth, green felt, basketball, flocked paper, silver gold, brown tile, glass tile, blue-black-gold tile, crinkle paper, and basketweave.

and its corresponding standard deviation, summarized in Table 1 ($MEMD_{\max} = 255$), that shows significantly larger spectral error for large $\kappa(256) \geq 3$ values for silver gold, flocked paper, mica, and basketweave. 2D random field models can approximate all other materials after the KLT decorrelation with an acceptably minor spectral error.

6   CONCLUSIONS

We presented a criterion allowing us to predict when a vast BTF data space can be modeled using a set of 2D random field models $(\kappa(\cdot) < 3)$ instead of more demanding 3D random field models without significant loss of spectral quality. This quality prediction allows avoiding demanding computing experiments with both types of models, spectrally decorrelated 2D and fully correlated 3D as well as circumvent the main problem with still non-existent reliable texture quality criteria. These mathematical models represent attractive modeling alternatives offering extreme data compression as only tens parameters must be stored instead of the original acquired data. They can reconstruct BTF space, i.e., predict the material's visual appearance under unmeasured conditions and synthesize textures of arbitrary size without disturbing visual artifacts and with preserved overall visual impressions. On the other hand, they can only approximate original data, which may result in visual quality compromise.

We performed robust experiments involving random field BTF models, analyzing and synthesizing under

Model	mica Mean	mica STD	fine sand Mean	fine sand STD	coarse sand Mean	coarse sand STD	burlap Mean	burlap STD	cork Mean	cork STD	towel Mean	towel STD	green cloth Mean	green cloth STD	green felt Mean	green felt STD	basketball Mean	basketball STD
2D CAR	3%	9%	5%	2%	5%	4%	5%	2%	2%	1%	3%	1%	3%	1%	5%	2%	5%	4%
2D MA	10%	27%	11%	6%	10%	13%	8%	3%	4%	1%	6%	17%	5%	2%	11%	4%	10%	13%
2D MSAR	4%	10%	5%	2%	5%	2%	6%	2%	3%	1%	2%	1%	3%	1%	4%	1%	5%	2%
2D MMRF	4%	10%	5%	2%	5%	2%	6%	2%	3%	1%	2%	1%	3%	1%	4%	1%	5%	2%
2D PMRF	4%	10%	5%	2%	5%	2%	6%	2%	3%	1%	2%	1%	3%	1%	4%	1%	5%	2%
3D CAR	3%	9%	4%	2%	4%	4%	4%	2%	2%	1%	2%	1%	2%	1%	3%	1%	4%	4%
3D MA	4%	10%	5%	3%	5%	4%	4%	1%	2%	1%	3%	4%	2%	1%	5%	3%	5%	4%
3D MSAR	4%	10%	7%	3%	6%	5%	7%	4%	4%	2%	4%	2%	5%	2%	5%	1%	6%	5%
3D MMRF	4%	9%	5%	2%	5%	4%	6%	2%	3%	1%	3%	1%	4%	2%	5%	1%	5%	4%
3D PMRF	4%	9%	5%	2%	5%	4%	6%	2%	3%	1%	3%	1%	4%	2%	5%	1%	5%	4%
$\kappa(256)$	3.18		2.42		1.14		4.3e-02		1.87e-03		7.3e-03		8.9e-04		6.3e-02		1.14	

Model	flocked paper Mean	flocked paper STD	silver gold Mean	silver gold STD	brown tile Mean	brown tile STD	glass tile Mean	glass tile STD	blue-black -gold tile Mean	blue-black -gold tile STD	crinkle paper Mean	crinkle paper STD	basketweave Mean	basketweave STD	all materials Mean	all materials STD
2D CAR	5%	4%	8%	8%	4%	5%	1%	4%	3%	5%	1%	4%	9%	6%	4%	5%
2D MA	9%	6%	23%	22%	10%	19%	4%	19%	10%	19%	2%	12%	17%	10%	9%	15%
2D MSAR	5%	4%	10%	7%	4%	3%	1%	2%	4%	4%	1%	0%	11%	7%	4%	5%
2D MMRF	5%	4%	10%	8%	4%	2%	1%	2%	4%	4%	1%	0%	11%	7%	4%	5%
2D PMRF	5%	4%	10%	9%	4%	2%	1%	1%	4%	4%	1%	0%	11%	7%	5%	5%
3D CAR	4%	4%	8%	8%	3%	5%	1%	4%	3%	5%	1%	4%	8%	5%	4%	5%
3D MA	4%	3%	9%	9%	4%	5%	2%	6%	4%	6%	1%	6%	9%	6%	4%	6%
3D MSAR	6%	4%	9%	8%	4%	6%	2%	6%	4%	6%	1%	4%	11%	7%	5%	6%
3D MMRF	6%	5%	9%	9%	4%	5%	1%	4%	4%	5%	1%	4%	10%	7%	5%	5%
3D PMRF	6%	5%	9%	9%	4%	5%	1%	4%	4%	5%	1%	4%	10%	7%	5%	5%
$\kappa(256)$	18.8		91.9		7.33e-01		5.04e-07		2.07e-02		1.07e-05		3.70			

Table 1: Mean values and standard deviations percentual $MEMD^* = 100 * MEMD/MEMD_{\max}$ values error corresponding to the best-achieved results for individual models and materials.

various conditions. All synthesized data were compared with corresponding original ones using texture color composition criterion MEMD. Achieved results confirmed that BTF measurements of materials with a limited range of colors predicted with the $\kappa()$ criterion from one perpendicular illuminated and observed angle can be reliably reconstructed using a set of simpler 2D random field models. The only exception with tested models is the oversimplified 2D MA model, which has mostly poor spectral performance.

Results of multidimensional textures related research are also applicable in medical applications and varied image processing problems, such as image restoration, cultural heritage preservation. BTF data are useful in a study of shadow casting by material structure and the analysis of material dimensionality. Analysis of different BTF samples can help understand human perception of real-world materials.

7 REFERENCES

[Ben97a] Bennett, J. Modeling and Analysis of Gray Tone, Color, and Multispectral Texture Images by Random Field Models and Their Generalizations, Ph.D. thesis, Southern Methodist University, Dallas, 1997.

[Ben98a] Bennett, J., Khotanzad, A. Multispectral Random Field Models for Synthesis and Analysis of Color Images. IEEE Transactions on Pattern Analysis and Machine Intelligence, 20, (3), pp. 327–332, 1998.

[Col73a] Cole Jr., H. A. On-line Failure Detection and Damping Measurement of Aerospace Structures by Random Decrement Signatures. Technical Report TMX-62.041, NASA, 1973.

[Cul04a] Cula, O., Dana, K., Murphy, F., Rao, B. Bidirectional Imaging and Modeling of Skin Texture. IEEE Transactions on Biomedical Engineering, 51, 12, pp.2148-2159, 2004.

[Dan97a] Dana, K., Nayar, S., van Ginneken, B., Koenderink, J. Reflectance and Texture of Real-World Surfaces. Proceedings of IEEE Conference Computer Vision and Pattern Recognition, pp.151-157, 1997.

[Fil18a] Filip, J., Kolafová, M., Havlíček, M., Vávra, R., Haindl, M., Rushmeier, H. Evaluating Physical and Rendered Material Appearance. The Visual Computer, 34, Springer (Computer Graphics International 2018), pp.805-816, 2018.

[Fil08a] Filip, J., Chantler, M., Green, P., Haindl, M. A Psychophysically Validated Metric for Bidirectional Texture Data Reduction. ACM Transactions on Graphics, 27, (5), 2008.

[Gri09a] Grim, J., Somol, P., Haindl, M., Daneš, J. Computer-Aided Evaluation of Screening Mammograms Based on Local Texture Models. IEEE Transactions on Image Processing, 18, (4), pp.765-773, 2009.

[Hai14a] Haindl, M., Kudělka, M. Texture fidelity benchmark. in Computational Intelligence for Multimedia Understanding (IWCIM), 2014 International Workshop on, IEEE Computer Society CPS, Los Alamitos, pp.1-5, 2014.

[Hai91a] Haindl, M. Texture Synthesis. CWI Quarterly, 4, (4), pp.305-331, 1991.

[Hai13a] Haindl, M., Filip, J. Visual Texture. Advances in Computer Vision and Pattern Recognition, Springer-Verlag, London, (2013).

[Hai02a] Haindl, M., Filip, J. Fast Restoration of color Movies Scratches. Proceedings of the 16th International Conference on Pattern Recognition, IEEE Computer Society, pp.269-272, 2002.

[Hai12a] Haindl, M., Havlíček, M. Bidirectional Texture Function Simultaneous Autoregressive Model. Computational Intelligence for Multimedia Understanding, pp.149-159, 2012.

[Hai02c] Haindl, M., Havlíček, V. A Multiscale color Texture Model. Proceedings of the 16th International Conference on Pattern Recognition, IEEE Computer Society, Los Alamitos, pp.255-258, 2002.

[Hai06a] Haindl, M., Vácha, P. Illumination Invariant Texture Retrieval. Proceedings of the 18th International Conference on Pattern Recognition, ICPR 2006, 3, IEEE Computer Society, pp.276-279, 2006.

[Hai07a] Haindl, M., Mikeš, S., Scarpa, G. Unsupervised Detection of Mammogram Regions of Interest. Knowledge-Based Intelligent Information and Engineering Systems. LNAI, 4694, Springer Berlin, pp.33-40, 2007.

[Hai08b] Haindl M., Mikeš, S. Unsupervised Mammograms Segmentation. Proceedings of the 19th International Conference on Pattern Recognition, ICPR 2008, IEEE Computer Society, Los Alamitos, pp.1-4, 2008.

[Has11a] Hasegawa, T., Tsumura, N., Nakaguchi, T., Iino, K. Photometric Approach to Surface Reconstruction of Artist Paitings. Journal of Electronic Imaging, 20, (1), 2011.

[HFV12a] Haindl, M., Filip, J., Vávra, R. Digital Material Appearance: the Curse of Tera-Bytes. ERCIM News, 90, pp.49-50, 2012.

[Hai23a] Haindl M. Bidirectional Texture Function Modeling, Handbook of Mathematical Models and Algorithms in Computer Vision and Imaging, Springer International Publishing, pp. 1023–1064, 2023.

[Hav12a] Havlíček, M. Bidirectional Texture Function Three Dimensional Pseudo Gaussian Markov Random Field Model. Doktorandské dny 2012, ČVUT, pp.53-62, 2012.

[Hav15a] Havlíček, M. Extended Bidirectional Texture Function Moving Average Model. Doktorandské dny 2015, ČVUT, pp.37-43, 2015.

[Hav19a] Havlíček, M., Haindl, M. Texture spectral similarity criteria. IET Image Processing, 13(11), pp.1998-2007, 2019.

[Hav21a] Havlíček, M., Haindl, M. Optimized Texture Spectral Similarity Criteria. Advances in Computational Collective Intelligence, Springer International Publishing, Cham, pp.644-655, 2021.

[Hav23a] Havlíček, M., Haindl, M. Texture Spectral Similarity Criteria Comparison. WSCG 2023 Proceedings - 31. International Conference in Central Europe on Computer Graphics, Visualization and Computer Vision WSCG 2023, University of West Bohemia, Plzeň, pp.100-106, 2023.

[Li92a] Li, X., Cadzow, J., Wilkes, D., Peters, R., Bodruzzaman II, M. An Efficient Two Dimensional Moving Average Model for Texture Analysis and Synthesis. Proceedings IEEE Southeastcon 1992, 1, pp.392-395, 1992.

[Mal01a] Malzbender, T., Gelb, D., Wolters, H. Polynomial Texture Maps. ACM SIGGRAPH 2001, ACM Press, pp.519-528, 2001.

[Sca09a] Scarpa, G., Haindl, M., Zerubia, J. Hierarchical Multiple Markov Chain Model for Unsupervised Texture Segmentation. IEEE Trans. on Image Processing, 18, (8), pp.1830-1843, 2009.

[Vac10a] Vácha, P., Haindl, M. Content-Based Tile Retrieval System. Structural, Syntactic, and Statistical Pattern Recognition, Lecture Notes in Computer Science, 6218, Springer Berlin/Heidelberg, pp.434-443, 2010.

[Vac09a] Vácha, P., Haindl, M. Illumination Invariant and Rotational Insensitive Textural Representation. Proceedings of IEEE Int. Conf. on Image Processing, ICIP, pp.1333-1336, 2009.

[Wan09a] Wang, Z., Simoncelli, E. P. Translation Insensitive Image Similarity in Complex Wavelet Domain. Proceedings of IEEE International Conference on Acoustics, Speech, and Signal Processing, pp.573-576, 2009.

[Zuj13a] Zujovic, J., Pappas, T., Neuhoff, D. Structural Texture Similarity Metrics for Image Analysis and Retrieval. IEEE Transactions on Image Processing, 22, (7), pp.2545-2558, 2013.